

# Core-shell nanoparticles based on an oxide metal: $\text{ReO}_3@Au$ (Ag) and $\text{ReO}_3@SiO_2$ ( $TiO_2$ )†

Sandeep Ghosh,<sup>ab</sup> Kanishka Biswas<sup>ab</sup> and C. N. R. Rao<sup>\*ab</sup>

Received 25th January 2007, Accepted 5th March 2007

First published as an Advance Article on the web 19th March 2007

DOI: 10.1039/b701137g

Core-shell nanoparticles based on metallic  $\text{ReO}_3$  nanoparticles have been prepared for the first time. The nanoparticles with the metallic shell *viz.*  $\text{ReO}_3@Au$  and  $\text{ReO}_3@Ag$  were prepared by the reduction of metal salts over  $\text{ReO}_3$  nanoparticle seeds.  $\text{ReO}_3@SiO_2$  and  $\text{ReO}_3@TiO_2$  core-shell nanoparticles were prepared by the hydrolysis of the organometallic precursors over the  $\text{ReO}_3$  nanoparticles. The core-shell nanoparticles have been characterized by transmission electron microscopy, optical absorption spectroscopy, energy dispersive X-ray spectroscopy, X-ray diffraction and Raman spectroscopy. The  $\text{ReO}_3@Au$  and  $\text{ReO}_3@Ag$  core-shell nanoparticles show composite plasmon absorption bands comprising contributions from both  $\text{ReO}_3$  and Au (Ag) whereas  $\text{ReO}_3@SiO_2$  and  $\text{ReO}_3@TiO_2$  show shifts in the plasmon bands depending on the refractive index of the shell material.

## Introduction

Core-shell nanoparticles constitute an important group of nanomaterials. Core-shell nanoparticles involving metallic nanoparticle cores and shells of oxides, semiconductors and other metals have been prepared and characterized. Similarly, core-shell particles with metal oxide cores and metallic oxide shells have also been synthesized and characterized. A variety of synthetic procedures have been employed for the synthesis of core-shell structures<sup>1</sup> which include precipitation,<sup>2,3</sup> micro-emulsion, reverse micelles,<sup>4-6</sup> sol-gel condensation,<sup>7</sup> layer-by-layer adsorption<sup>8,9</sup> and graft polymerization.<sup>10</sup> Among the various core-shell particles those containing cores of metals such as Au and Ag form a majority and there are a large number of papers in this area for example core-shell particles of the type  $Ag@Au$ ,<sup>11</sup>  $Au@Ag$ <sup>12,13</sup> have been prepared and their properties reported. Similarly, core-shell particles of the kind  $Au@SiO_2$ ,<sup>14</sup>  $Au@SnO_2$ ,<sup>15</sup>  $Au@TiO_2$ <sup>16-19</sup> and  $Fe_3O_4@Au$ <sup>20</sup> have also been characterized by various techniques. Recently, nanoparticles of  $\text{ReO}_3$  which is a good metal have been prepared and characterized.<sup>21</sup> Since  $\text{ReO}_3$  is a metal which looks like copper and conducts like copper, we considered it important to investigate core-shell nanostructures formed with such an oxide metal as the core, with the noble metals and metal oxides as shell materials. It is noteworthy that  $\text{ReO}_3$  gives rise to a plasmon band in the visible region just like gold and copper. Core-shell particles comprising such  $\text{ReO}_3$  cores may indeed be useful as sensors and other applications. In this article, we describe the synthesis and properties of novel core-shell particles based on  $\text{ReO}_3$

nanocrystals. The systems studied include  $\text{ReO}_3@Au$ ,  $\text{ReO}_3@Ag$ ,  $\text{ReO}_3@SiO_2$  and  $\text{ReO}_3@TiO_2$ .

## Experimental

The preparation of the  $\text{ReO}_3$ -based core-shell nanoparticles involved a two-stage synthetic methodology. The first step involved the synthesis of the  $\text{ReO}_3$  nanoparticles following the procedure reported by us elsewhere<sup>21</sup> and the second involved the use of these nanoparticles as seeds in various reaction solutions containing the precursor for the shell-material and subsequently reducing (in the case of gold and silver) or hydrolyzing (in the case of  $TiO_2$  and  $SiO_2$ ) the shell-material over the  $\text{ReO}_3$  nanoparticles.

The synthesis of  $\text{ReO}_3$  nanoparticles involves the preparation of the rhenium(VII) oxide-dioxane complex,  $\text{Re}_2O_7-(C_4H_8O_2)_x$  as the starting material (following the literature procedure<sup>22,23</sup>) and its solvothermal decomposition in toluene to yield the desired nanoparticles. In a typical synthesis, 0.025 g (0.12 mmol) of  $\text{Re}_2O_7$  was taken in a 10 mL round-bottomed flask and 0.25 mL (2.93 mmol) of anhydrous 1,4-dioxane was added to it. This mixture was warmed in a water bath maintained at 70 °C and then frozen in an ice bath alternatively until rhenium(VII) oxide-dioxane complex (RDC) precipitated out as a dense, pearl gray deposit. The complex was dissolved in 2 mL (30.08 mmol) of ethanol and was taken in 45 mL of toluene and sealed in a Teflon-lined stainless steel autoclave of 80 mL capacity (at 70% filling fraction). It was then heated at 200 °C for 4 hours. The red  $\text{ReO}_3$  nanoparticles (12 nm diameter) were washed several times with acetone. The particle size of  $\text{ReO}_3$  could be increased by increasing the RDC concentration keeping the amount of toluene and the filling fraction of the autoclave constant. XRD patterns show the  $\text{ReO}_3$  nanoparticles to be crystalline with a cubic structure (space group  $Pm\bar{3}m$ ,  $a = 3.748 \text{ \AA}$ , JCPDS-00-24-1009).<sup>21</sup> The dried  $\text{ReO}_3$  particles could be readily redispersed in ethanol or DMF.

<sup>a</sup>Chemistry and Physics of Materials Unit, DST unit on Nanoscience and CSIR Centre of Excellence in Chemistry, Jawaharlal Nehru Centre for Advanced Scientific Research, Jakkur P.O., Bangalore-560064, India.

E-mail: cnrao@jncasr.ac.in; Fax: +91 80 22082760

<sup>b</sup>Solid State and Structural Chemistry Unit, Indian Institute of Science, Bangalore-560012, India

† The HTML version of this article has been enhanced with colour images.

For the synthesis of  $\text{ReO}_3@Au$  core-shell particles, auric ions were reduced over  $\text{ReO}_3$  seeds following a modification of the method of Enüstün and Turkevich.<sup>24</sup> A stock solution of  $10^{-2}$  M  $\text{HAuCl}_4$  in ethanol was prepared and used subsequently for the reactions. Although ethanol solutions themselves are quite stable, the  $\text{HAuCl}_4$  "stock" solution in ethanol was prepared afresh for each series of reactions and was not stored to avoid any reduction. For the preparation of core-shell nanoparticles, the  $\text{ReO}_3 : Au$  molar ratio was kept at 1 : 2 and 1 : 4 and the amount of  $\text{ReO}_3$  to be added to the reaction solution calculated accordingly *viz.* 3 mg and 1.5 mg of  $\text{ReO}_3$  nanoparticles for the 1 : 2 and 1 : 4 reactions, respectively (keeping the  $\text{HAuCl}_4$  concentration constant). In a typical synthesis, 100 ml of the  $\text{HAuCl}_4$  stock solution containing the  $\text{ReO}_3$  seeds was sonicated for 20 minutes (to disperse the  $\text{ReO}_3$  nanoparticles). To the reaction mixture was then added 1.5 ml of 1% aqueous trisodium citrate solution dropwise with stirring. The solution was allowed to stir overnight. The nanoparticles so formed precipitated out of the solution and were collected aided by centrifugation. The nanoparticles were washed several times with ethanol.

For the synthesis of  $\text{ReO}_3@Ag$  core-shell particles,  $\text{Ag}^+$  ions were reduced over  $\text{ReO}_3$  seeds by the procedure of Lee and Meisel.<sup>25</sup> A stock solution of  $10^{-3}$  M  $\text{AgNO}_3$  in water was prepared and used subsequently for the reactions. For the preparation of core-shell nanoparticles, the  $\text{ReO}_3 : Ag$  molar ratio was kept at 1 : 2 and 1 : 3 and the amount of  $\text{ReO}_3$  to be used in the reaction was kept constant at 5 mg per reaction whereas the volume of the  $\text{AgNO}_3$  aqueous solution and the volume of the 1% trisodium citrate solution to be added was calculated accordingly. In a typical synthesis, 5 mg of  $\text{ReO}_3$  was dispersed in 30 ml of ethanol aided by sonication for 20 minutes and then to this solution was added the calculated amount of  $\text{AgNO}_3$  stock solution (43 ml for 1 : 2 particles and 86 ml for the 1 : 4 particles). To this was added 1% aqueous trisodium citrate solution (0.86 ml for 1 : 2 and 1.72 ml for 1 : 4) dropwise with stirring. The solution was allowed to stir overnight. The nanoparticles so formed precipitated out of the solution and were collected aided by centrifugation. The nanoparticles were washed several times with ethanol.

For the synthesis of  $\text{ReO}_3@SiO_2$  core-shell particles, tetraethylorthosilicate (TEOS) was hydrolyzed over  $\text{ReO}_3$  seeds by using the method reported by Stöber *et al.*<sup>26</sup> The amount of  $\text{ReO}_3$  nanoparticles was kept constant at 5 mg per reaction while the amount of TEOS was varied accordingly so that the  $\text{ReO}_3 : SiO_2$  molar ratio comes to 1 : 2, 1 : 3 and 1 : 4. A solution of ethanol : water : ammonium hydroxide = 98 : 31 : 4 was prepared and sonicated with  $\text{ReO}_3$  nanoparticles for 20 minutes to obtain a uniform solution. To this was added the TEOS (in ethanol) dropwise with stirring. The solution was allowed to stir overnight. The solution assumed a faint yellow tinge (a change in colour from the dark green colour of  $\text{ReO}_3$  dispersion) and the colour of the solution deepened with the increase in the silica content.

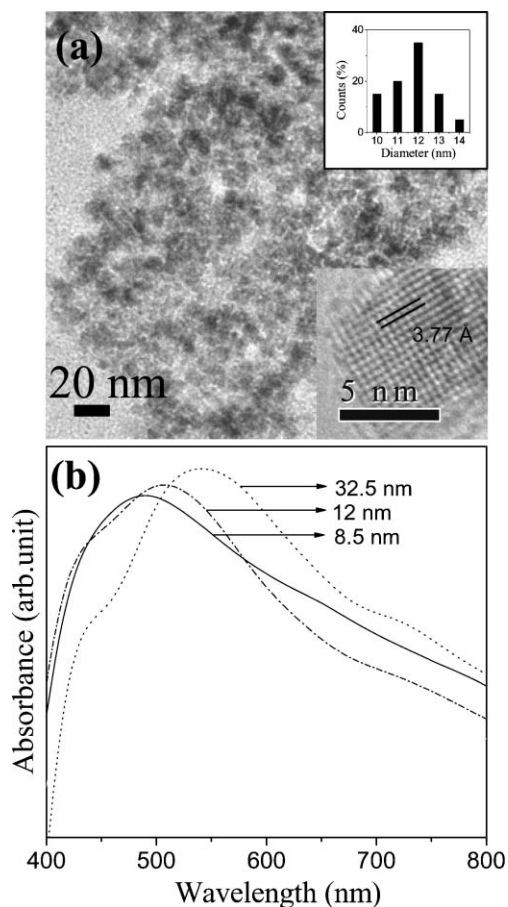
For the synthesis of  $\text{ReO}_3@TiO_2$  core-shell particles, titanium tetra(*n*-butoxide) (TOB) was hydrolyzed over  $\text{ReO}_3$  using a modification of the procedure reported by Scolan and Sanchez.<sup>27</sup> The amount of  $\text{ReO}_3$  was kept constant at 5 mg per reaction whereas the amount of TOB was varied accordingly

to keep the molar ratio of  $\text{ReO}_3 : TiO_2$  at 1 : 2 and 1 : 4. Two solutions were prepared for a typical reaction: one containing 5 mg of  $\text{ReO}_3$  and 0.8 M  $H_2O$  in dimethylformamide (DMF) and the other comprising of equimolar amounts of TOB and acetylacetone in ethanol in a concentration of 5.75 mM each. Both the solutions were sonicated for 20 minutes each to obtain clear mixtures and then the TOB containing solution was added to the  $\text{ReO}_3$  solution dropwise with stirring while heating at 80 °C. After 90 minutes the colour of the solution changes from the dark green colour of  $\text{ReO}_3$  to light yellow and this colour deepened with the increase of the titania content.

The core-shell nanoparticles were characterized by transmission electron microscopy (TEM), optical absorption spectroscopy, energy dispersive X-ray spectroscopy (EDAX), X-ray diffraction (XRD) and Raman spectroscopy. Core-shell nanoparticles were repeatedly prepared by the procedures described above to collect sufficient samples for characterization. For transmission electron microscopy, ethanol dispersions of the nanoparticles were taken on holey carbon-coated Cu grids, and the grids dried in air. The grids were examined using a JEOL (JEM3010) microscope operating with an accelerating voltage of 300 kV. Electronic absorption spectra were recorded using a Perkin-Elmer spectrometer. Powder X-ray diffraction patterns for the nanoparticles were obtained using a Philips X'Pert diffractometer employing the Bragg-Brentano configuration. The EDAX spectra were recorded using a LEICA S440i SEM. Raman spectra for the metal oxide coated particles were recorded using LabRAM HR800 using 632 nm laser as the excitation source.

## Results and discussion

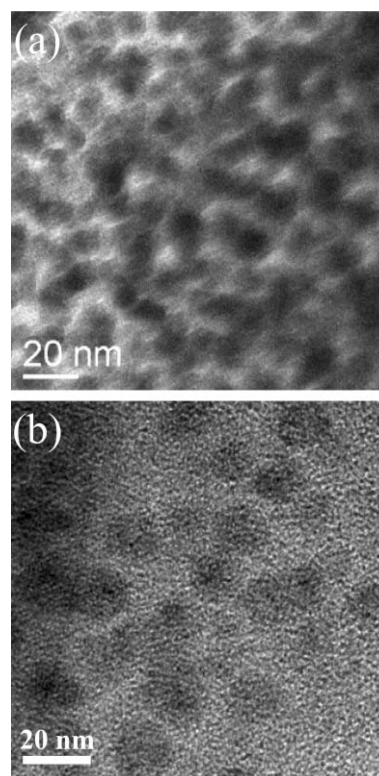
We prepared  $\text{ReO}_3$  nanoparticles in the diameter range of 8.5–32.5 nm by the decomposition of the  $\text{Re}_2O_7$ -dioxane complex under solvothermal conditions. In Fig. 1(a), we show a TEM image of the  $\text{ReO}_3$  nanoparticles with an average diameter of 12 nm. The size distribution histogram (shown as upper inset in Fig. 1(a)) shows that the particles are reasonably monodisperse with the diameters varying between 10 nm and 14 nm. The lower inset in Fig. 1(a) shows a high-resolution electron microscope image of an 8.5 nm particle. The 8.5 nm particle shown here was obtained from a separate preparation and does not correspond to the TEM images of Fig. 1(a). The lattice spacing of 3.77 Å corresponds to the (100) interplanar distance in the  $\text{ReO}_3$  crystals.  $\text{ReO}_3$  is known to exhibit a plasmon absorption band in the visible region just like gold and copper.<sup>28</sup> It is well known that the surface plasmon resonance is the coherent excitation of the free electrons within the conduction band, leading to an in-phase oscillation.<sup>29</sup> The surface obviously plays an important role for the polarizability of the metal and therefore shifts the resonance to optical frequencies. In Fig. 1(b), we show the electronic absorption spectra of the  $\text{ReO}_3$  nanoparticles prepared by us. It is evident from the spectra that the  $\lambda_{\text{max}}$  of the absorption band shifts to the lower wavelengths with the decrease in the particle size. The  $\lambda_{\text{max}}$  values for the 32.5, 12 and 8.5 nm nanocrystals are 543, 507 and 488 nm respectively. Such a blue-shift of the surface plasmon band with decreasing particle size occurs in



**Fig. 1** (a) TEM image of  $\text{ReO}_3$  nanocrystals with an average diameter of 12 nm. Upper inset shows the size distribution histogram and the lower one shows the single particle HREM image of the 8.5 nm particle, (b) UV-visible spectra of  $\text{ReO}_3$  nanocrystals with average diameters of 8.5, 12 and 32.5 nm.

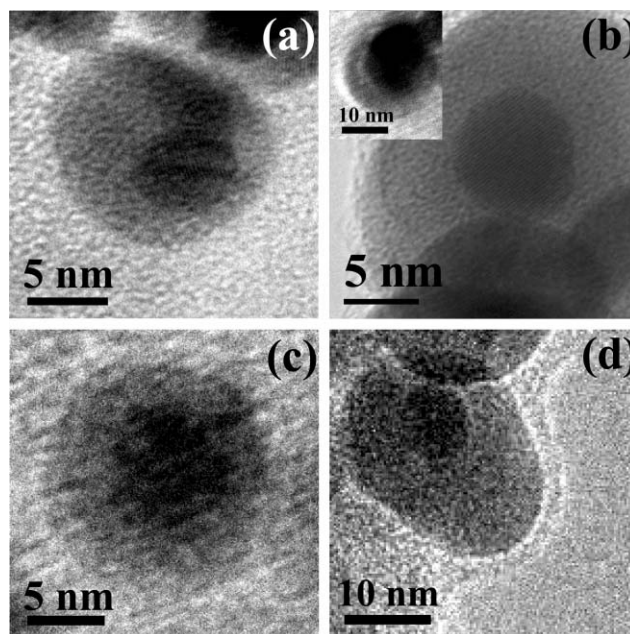
gold nanoparticles as well.<sup>30</sup> The surface of  $\text{ReO}_3$  nanoparticles could readily adsorb organic molecules such as pyridine, pyrazine and pyrimidine. Evidence for bonding between the surface of the  $\text{ReO}_3$  nanoparticles and the adsorbed molecules has been found by surface enhanced Raman scattering effect of pyridine, pyrazine and pyrimidine on the surfaces of  $\text{ReO}_3$  nanoparticles. Thus, Raman bands of all these aza-aromatics adsorbed on  $\text{ReO}_3$  surface show red-shift and large intensification compared to pure analyte Raman band.<sup>31</sup>

The various core-shell nanoparticles prepared by us were characterized by TEM. In Figs. 2(a) and (b), we show typical low-magnification TEM images in the case of  $\text{ReO}_3@Ag$  and  $\text{ReO}_3@SiO_2$  core-shell nanoparticles. The particles are reasonably dispersed. In Figs. 3(a) and (b), we show the TEM images of the  $\text{ReO}_3@Au$  core-shell nanoparticles in which the Au shell is formed over  $\text{ReO}_3$  nanoparticles of three different sizes. The core-shell nanoparticle in Fig. 3(a) is formed over a 5 nm  $\text{ReO}_3$  particle. The core-shell nanoparticles in Fig. 3(b) are formed over 8 nm and 12 nm  $\text{ReO}_3$  particles. The XRD pattern of the core-shell nanoparticles (see Fig. 4 (a)) matches with that of cubic gold (space group  $Fm\bar{3}m$ ,  $a = 4.07 \text{ \AA}$ , JCPDS-00-001-1172) establishing the presence of gold. For reasons not entirely clear to us, we did not find any reflections

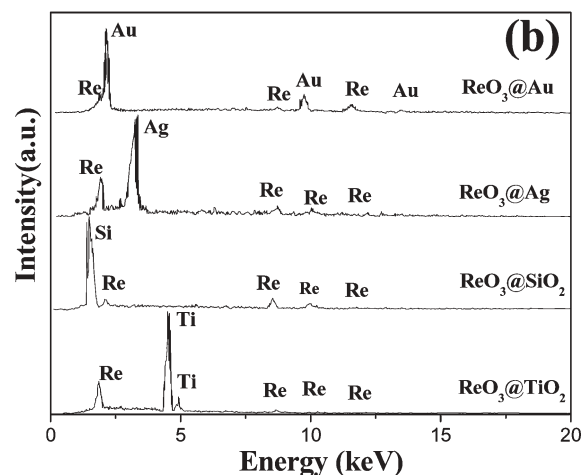
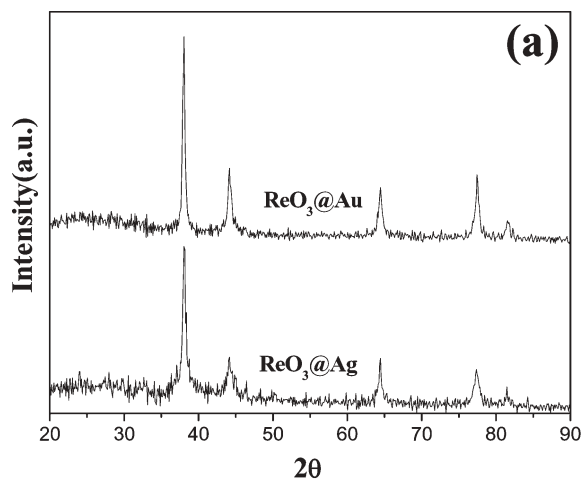


**Fig. 2** TEM images of (a)  $\text{ReO}_3@Ag$  nanoparticles, and (b)  $\text{ReO}_3@SiO_2$  nanoparticles.

of  $\text{ReO}_3$  in the XRD patterns of the core-shell nanoparticles although the  $\text{ReO}_3$  nanoparticles were crystalline. However, EDAX analysis (Fig. 4(b)) shows the presence of both rhenium



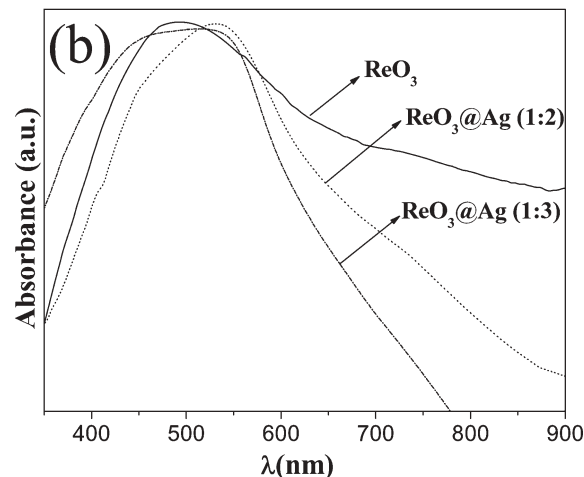
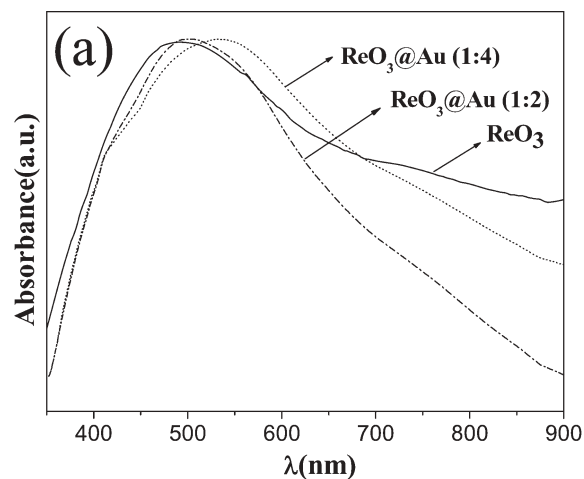
**Fig. 3** TEM images of core-shell nanoparticles of (a)  $\text{ReO}_3@Au$  formed with a 5 nm  $\text{ReO}_3$  particle, (b)  $\text{ReO}_3@Au$  formed over an 8 nm  $\text{ReO}_3$  particle; the inset showing a core-shell nanoparticle formed over a 12 nm  $\text{ReO}_3$  particle, (c)  $\text{ReO}_3@Ag$  formed over a 5 nm  $\text{ReO}_3$  particle, and (d)  $\text{ReO}_3@Ag$  formed over an 8 nm particle of  $\text{ReO}_3$ .



**Fig. 4** (a) XRD patterns of  $\text{ReO}_3@Au$  and  $\text{ReO}_3@Ag$  core-shell nanoparticles, (b) EDAX spectra of  $\text{ReO}_3@Au$ ,  $\text{ReO}_3@Ag$ ,  $\text{ReO}_3@SiO_2$  and  $\text{ReO}_3@TiO_2$  core-shell nanoparticles.

and gold. Fig. 5(a) shows the UV-visible absorption spectra of  $\text{ReO}_3@Au$  core-shell nanoparticles with  $\text{ReO}_3 : Au$  ratios of 1 : 2 and 1 : 4. The spectra represent composite bands comprising the plasmon absorption bands of  $\text{ReO}_3$  and Au. Note that the plasmon band of the  $\text{ReO}_3$  nanocrystals is around 500 nm while that of bulk gold is around 520 nm. This is the reason why the band shifts to longer wavelengths with increase in gold content of the shell. As the quantity of the shell precursor is increased, the shell thickness increases. Thus, an average shell thickness of  $\sim 3$  nm was obtained in the case of  $\text{ReO}_3@Au$  core-shell nanoparticles when the  $\text{ReO}_3 : Au$  molar ratio was 1 : 2, but increased to  $\sim 5$  nm when the  $\text{ReO}_3 : Au$  molar ratio was increased to 1 : 4.

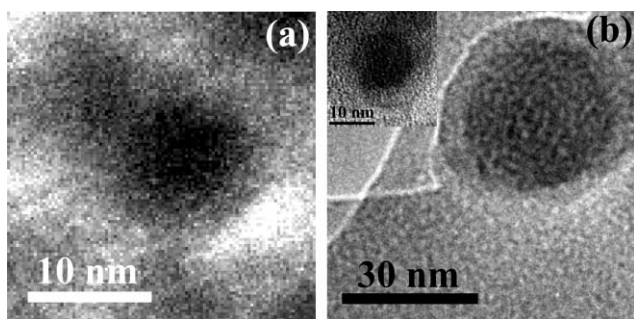
TEM images of  $\text{ReO}_3@Ag$  core-shell nanoparticles are shown in Figs. 3(c) and (d) wherein the  $\text{ReO}_3$  core particles have diameters of 5 nm and 8 nm respectively. The shell thickness obtained in case of  $\text{ReO}_3@Ag$  core-shell nanoparticles was  $\sim 4$  nm when the  $\text{ReO}_3 : Ag$  molar ratio was 1 : 2, and  $\sim 6$  nm when the  $\text{ReO}_3 : Ag$  molar ratio was 1 : 3. The XRD pattern (Fig. 4(a)) of the core-shell nanoparticles matches with that of cubic silver (space group  $Fm\bar{3}m$ ,  $a = 4.079 \text{ \AA}$ , JCPDS-00-001-1164). The EDAX spectrum in Fig. 4(b) shows the presence of both rhenium and silver. The



**Fig. 5** UV-vis absorption spectra of (a)  $\text{ReO}_3@Au$  core-shell nanoparticles (1 : 2 and 1 : 4) with a 12 nm  $\text{ReO}_3$  particle, and (b)  $\text{ReO}_3@Ag$  core-shell nanoparticles (1 : 2 and 1 : 3) with a 12 nm  $\text{ReO}_3$  particle.

UV-visible absorption spectra of  $\text{ReO}_3@Ag$  core-shell nanoparticles with ratios of 1 : 2 and 1 : 3 are shown in Fig. 5(b). These spectra also represent composite bands comprising the plasmon absorption bands of  $\text{ReO}_3$  and Ag. The plasmon absorption band of bulk Ag is around 420 nm. As such, we observe the broad plasmon bands shifting to lower wavelengths with increase in Ag content of the shell.

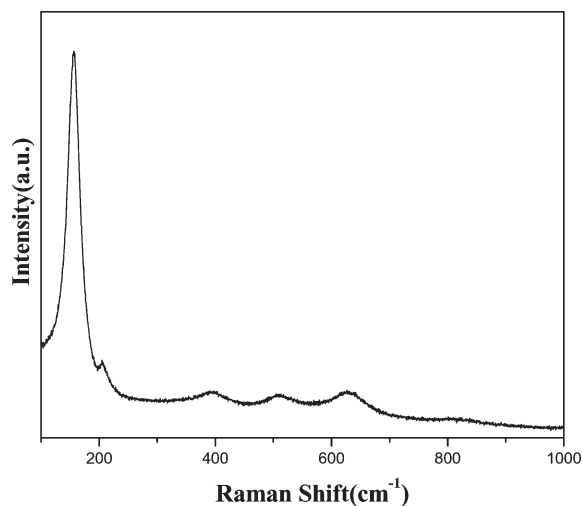
Fig. 6(a) shows a TEM image of a  $\text{ReO}_3@SiO_2$  core-shell nanoparticle formed over an 8.5 nm  $\text{ReO}_3$  particle. A shell thickness of  $\sim 4$  nm was obtained for these core-shell nanoparticles when the  $\text{ReO}_3 : SiO_2$  molar ratio was 1 : 2. The shell thickness increased as the silica content was increased. The UV-visible absorption spectrum, shown in Fig. 7(a) shows a blue-shift of the  $\text{ReO}_3$  plasmon band towards shorter wavelengths with increase in the  $SiO_2$  content. The presence of  $SiO_2$  as the shell material is confirmed by the EDAX analysis as can be seen from Fig. 4(b) which shows the presence of both rhenium and silicon. Fig. 7(b) shows photographs of the solutions of  $\text{ReO}_3@SiO_2$  core-shell particles in ethanol revealing that the colour of the solution deepens as the proportion of  $SiO_2$  is increased. Thus the formation of the  $\text{ReO}_3@SiO_2$  core-shell particles can be



**Fig. 6** (a) TEM image of a  $\text{ReO}_3@SiO_2$  core-shell nanoparticle formed over an 8.5 nm  $\text{ReO}_3$  particle, and (b) TEM image of a  $\text{ReO}_3@TiO_2$  core-shell nanoparticle formed over a 32 nm  $\text{ReO}_3$  particle with the inset showing a core-shell nanoparticle formed over a 12 nm particle of  $\text{ReO}_3$ .

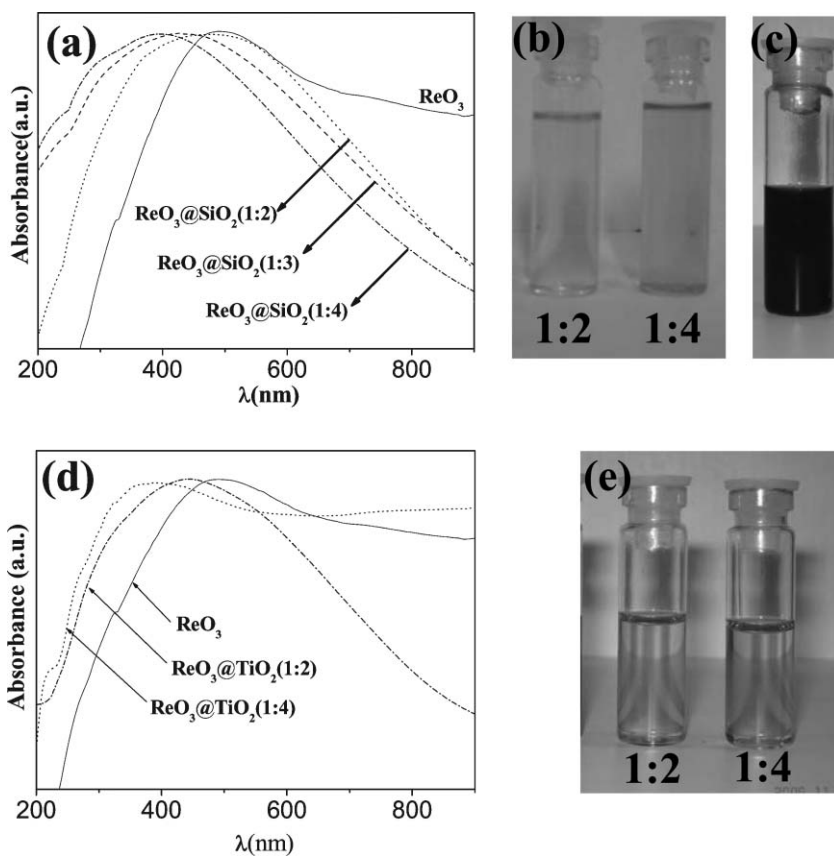
visualized by the colours of the solutions of the nanoparticles in ethanol (Fig. 7(c)).

Fig. 6(b) shows TEM images of  $\text{ReO}_3@TiO_2$  core-shell particles formed over 32 nm and 12 nm  $\text{ReO}_3$  nanoparticles. The core-shell structure is confirmed by the EDAX analysis as shown in Fig. 4(b) which shows the presence of both rhenium and titanium. Raman spectrum of  $\text{ReO}_3@TiO_2$  core-shell nanoparticles (Fig. 8) indicate that  $TiO_2$  has the anatase



**Fig. 8** Raman spectrum of  $\text{ReO}_3@TiO_2$  core-shell nanoparticles.

structure (although the sample is amorphous from the XRD) with characteristic bands at 138, 393, 514 and  $636\text{ cm}^{-1}$ .<sup>32</sup> The UV-visible absorption spectra show a behavior similar to that of  $\text{ReO}_3@SiO_2$  core-shell nanoparticles (Fig. 7(d)). Thus, the plasmon band is blue-shifted towards shorter wavelengths with increase in  $TiO_2$  content. In case of  $TiO_2$  coating, the shell



**Fig. 7** (a) UV-vis absorption spectra of  $\text{ReO}_3@SiO_2$  core-shell nanoparticles (1 : 2, 1 : 3 and 1 : 4), (b) photograph of the solutions of  $\text{ReO}_3@SiO_2$  nanoparticles in ethanol in different molar ratios (1 : 2 and 1 : 4), (c) photograph of  $\text{ReO}_3$  nanoparticle solution in ethanol, (d) UV-vis absorption spectra of  $\text{ReO}_3@TiO_2$  core-shell nanoparticles (1 : 2 and 1 : 4), and (e) photograph of  $\text{ReO}_3@TiO_2$  nanoparticles in DMF in different molar ratios (1 : 2 and 1 : 4).

thicknesses were  $\sim 5$  nm and  $\sim 8$  nm for  $\text{ReO}_3 : \text{TiO}_2$  molar ratios of 1 : 2 and 1 : 4, respectively. The blue-shift is larger in the case of  $\text{TiO}_2$  compared to  $\text{SiO}_2$ . This can be attributed to the higher refractive index of  $\text{TiO}_2$  ( $n = 2.49$  for anatase phase) compared to that of  $\text{SiO}_2$  ( $n = 1.45$ ). We show photographs of  $\text{ReO}_3@ \text{TiO}_2$  core-shell nanoparticles in dimethylformamide in Fig. 7(d).

The blue-shift of the plasmon bands of  $\text{ReO}_3@ \text{SiO}_2$  and  $\text{ReO}_3@ \text{TiO}_2$  nanoparticles is rather unusual. Normally, when shells with high refractive index form over metal cores such as Au, the plasmon band is shifted to longer wavelengths, the shift being proportional to the refractive index of the shell material. The blue-shift observed in this case is due to excess of  $\text{SiO}_2$  or  $\text{TiO}_2$  present in solution after deposition on the  $\text{ReO}_3$  nanoparticles, as pointed out earlier by Liz-Marzán.<sup>14</sup> The scattering from the medium is responsible for blue-shifting the plasmon absorption bands, the shift being higher in case of  $\text{TiO}_2$ .

## Conclusions

In conclusion, it is possible to prepare core-shell particles around a nanoparticle of an oxide metal such as  $\text{ReO}_3$  as the core. Thus, core-shell particles described here are indeed unique. The  $\text{ReO}_3@ \text{Au}$ ,  $\text{ReO}_3@ \text{Ag}$ ,  $\text{ReO}_3@ \text{SiO}_2$  and  $\text{ReO}_3@ \text{TiO}_2$  core-shell particles show spectra with the expected characteristics. It should be possible to prepare other core-shell nanoparticles with  $\text{ReO}_3$  as the core e.g.  $\text{ReO}_3@ \text{CdS}$  and  $\text{ReO}_3@ \text{CdSe}$ . These nanoparticles may find applications as sensors.

## References

- (a) Y. Xia, B. Gates, Y. Yin and Y. Lu, *Adv. Mater.*, 2000, **12**, 693; (b) V. Salgueiriño-Maceira and M. A. Correa-Duarte, *J. Mater. Chem.*, 2006, **16**, 3593.
- A. Imhof, *Langmuir*, 2001, **17**, 3579.
- M. Ocana, W. P. Hsu and E. Matijevic, *Langmuir*, 1991, **7**, 2911.
- T. Li, J. Moon, A. A. Morrone, J. J. Mecholsky, D. R. Talham and J. H. Adair, *Langmuir*, 1999, **15**, 4328.

- J. Lin, W. Zhou, A. Kumbhar, J. Wiemann, J. Fang, E. E. Carpenter and C. J. O'Connor, *J. Solid State Chem.*, 2001, **159**, 26.
- H. Huang, E. E. Remsen, T. Kowalewski and K. L. Wooley, *J. Am. Chem. Soc.*, 1999, **121**, 3805.
- K. H. See, M. E. Mullins, O. P. Mills and P. A. Heiden, *Nanotechnology*, 2005, **16**, 1950.
- F. Caruso, R. A. Caruso and H. Möhwald, *Chem. Mater.*, 1999, **11**, 3309.
- F. Caruso, M. Spasova, V. Salgueiriño-Maceira and L. M. Liz-Marzán, *Adv. Mater.*, 2001, **13**, 1090.
- M. Okaniwa, *J. Appl. Polym. Sci.*, 1998, **68**, 185.
- L. Rivas, S. Sanchez-Cortes, J. V. Garcia-Ramos and G. Morcillo, *Langmuir*, 2000, **16**, 9722.
- F. Hubenthal, T. Ziegler, C. Hendrich, M. Alschinger and F. Träger, *Eur. Phys. J. D*, 2005, **34**, 165.
- S. Bruzzone, G. P. Arrighini and C. Guidotti, *Mater. Sci. Eng., C*, 2000, **23**, 965.
- L. Liz-Marzán, M. Giersig and P. Mulvaney, *Langmuir*, 1996, **12**, 4329.
- G. Oldfield, T. Ung and P. Mulvaney, *Adv. Mater.*, 2000, **12**, 1519.
- I. Pastoriza-Santos, D. S. Koktysh, A. A. Mamedov, M. Giersig, N. A. Kotov and L. Liz-Marzán, *Langmuir*, 2000, **16**, 2731.
- K. S. Mayya, D. I. Gittins and F. Caruso, *Chem. Mater.*, 2001, **13**, 3833.
- S. K. Medda, S. De and G. De, *J. Mater. Chem.*, 2005, **15**, 3278.
- A. Dawson and P. V. Kamat, *J. Phys. Chem. B*, 2001, **105**, 960.
- L. Wang, J. Luo, Q. Fan, M. Suzuki, I. S. Suzuki, M. H. Engelhard, Y. Lin, N. Kim, J. Q. Wang and C. J. Zhong, *J. Phys. Chem. B*, 2005, **109**, 21593.
- K. Biswas and C. N. R. Rao, *J. Phys. Chem. B*, 2006, **110**, 842.
- H. Nechamkin, A. N. Kurtz and C. F. Hiskey, *J. Am. Chem. Soc.*, 1951, **73**, 2828.
- L. F. Audrieth, *Inorg. Synth.*, 1950, **3**, 187.
- B. V. Enüstün and J. Turkevich, *J. Am. Chem. Soc.*, 1963, **85**, 3317.
- C. Lee and D. Meisel, *J. Phys. Chem.*, 1982, **86**, 3391.
- W. Stöber, A. Fink and E. Bohn, *J. Colloid Interface Sci.*, 1968, **26**, 62.
- E. Scolan and C. Sanchez, *Chem. Mater.*, 1998, **10**, 3217.
- R. Edreva-Kardzhieva and A. A. Andreev, *Zh. Neorg. Khim.*, 1977, **22**, 2007.
- S. Link and M. A. El-Sayed, *Int. Rev. Phys. Chem.*, 2000, **19**, 409.
- S. Link and M. A. El-Sayed, *J. Phys. Chem. B*, 1999, **103**, 4212.
- K. Biswas, S. V. Bhat and C. N. R. Rao, *J. Phys. Chem.*, 2007, DOI: 10.1021/jp068894i.
- K. Lagarec and S. Desgreniers, *Solid State Commun.*, 1995, **94**, 519.